Journal of Porphyrins and Phthalocyanines
J. Porphyrins Phthalocyanines 2024; **28**: 300–307
DOI: 10.1142/S1088424624500263

Published at https://www.worldscinet.com/jpp/

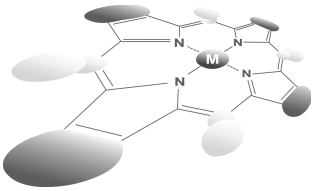

Finally: The X-ray crystal structure of the illusive unsubstituted iron(III) phthalocyanine μ-oxo(1) dimer. DFT-predicted Mössbauer quadrupole splitting and antiferromagnetic coupling constants for X-ray geometry

Victor N. Nemykin[a,◊,*], Nikolay N. Gerasimchuk[b] and Breanna E. Muldowney[a]

[a]*Department of Chemistry, University of Tennessee – Knoxville, Knoxville, TN, 37996, USA*
[b]*Department of Chemistry, Missouri State University, Springfield, MO, 65897, USA*

Received 14 May 2024
Accepted 15 May 2024

ABSTRACT: The molecular structure of the unsubstituted iron(III) phthalocyanine μ-oxo(1) dimer ($(PcFe)_2O$) was determined by single crystal X-ray diffraction. In agreement with the earlier speculations, the dimer has a bent (Fe-O-Fe angle is 152.4°) structure. The interplay between the π-π interactions and steric hindrances caused by the isoindole units led to the observed staggering angle of ~24° between two phthalocyanine ligands. The high-spin iron(III) centers are located significantly above the phthalocyanine N4 planes (0.57–0.58 Å). Several DFT exchange-correlation functionals were used to calculate the absolute value and sign of the Mössbauer quadrupole splitting and antiferromagnetic coupling constant for X-ray determined geometry of $(PcFe)_2O$. It was demonstrated that the hybrid functionals provide the correct sign of the electric field gradient and the magnitude of the antiferromagnetic coupling constant compared to the pure functionals.

KEYWORDS: iron, phthalocyanine, μ-oxo dimer, X-ray crystallography, DFT calculations.

INTRODUCTION

Iron phthalocyanines are a very interesting class of compounds that have diverse coordination, redox, and spin states [1]. In particular, iron(III) phthalocyanines form low-spin (s = 1/2) hexacoordinated complexes [2], spin-admixed (s = 3/2-5/2) pentacoordinated complexes [3], and penta- and hexacoordinated μ-oxo [4], μ-nitrido [5], and μ-carbido [6] dimers (Fig. 1). It has been shown that the pentacoordinated μ-oxo [7] and μ-nitrido [8] dimers can catalyze a large array of oxidative C-H transformations in the organic substrates including methane oxidation. It is known that the μ-oxo dimers of the general formula $(Pc^{Rn}Fe)_2O$ exist in two different isomer forms: μ-oxo(1) and μ-oxo(2) [4, 7, 9]. The crystal structures of the μ-oxo(2) form are known for unsubstituted phthalocyanine (refined from the powder ADXD/EDXD X-ray diffraction data and reported by Ercolani and co-workers) [10] and fluorinated phthalocyanine, $Pc^{(\alpha\text{-}CF3)8}Fe)_2O$, reported by Gorun and co-workers [11] (Fig. 1). In both cases, the linear Fe-O-Fe arrangement of the central core was observed. The electronic structures of the μ-oxo(1) and μ-oxo(2) isomers were probed by UV-Vis, ^{1}H NMR, IR, Mössbauer, and UV-Vis spectroscopy as well as magnetochemistry [4, 7, 9]. Recently, we have explored the solution chemistry and redox properties of the soluble $(Pc^{tBu4}Fe)_2O$ complex and shown that μ-oxo(1) is the only stable isomer in non-coordinating solvents [12]. Despite the recent progress in the chemistry and electronic structure of the μ-oxo species that have been known for more than 40 years, there are no crystal structures of the μ-oxo(1) species are known and thus, the bent structure of the μ-oxo(1) dimer remains speculative. Thus, in this paper, we report the first example of the X-ray structure of the unsubstituted μ-oxo(1) complex and use DFT calculations to confirm its Mössbauer quadrupole splitting sign and amplitude as well as the magnitude of the antiferromagnetic coupling between two iron centers.

◊SPP full member in good standing.

*Correspondence to: Victor N. Nemykin, e-mail: vnemykin@utk.edu

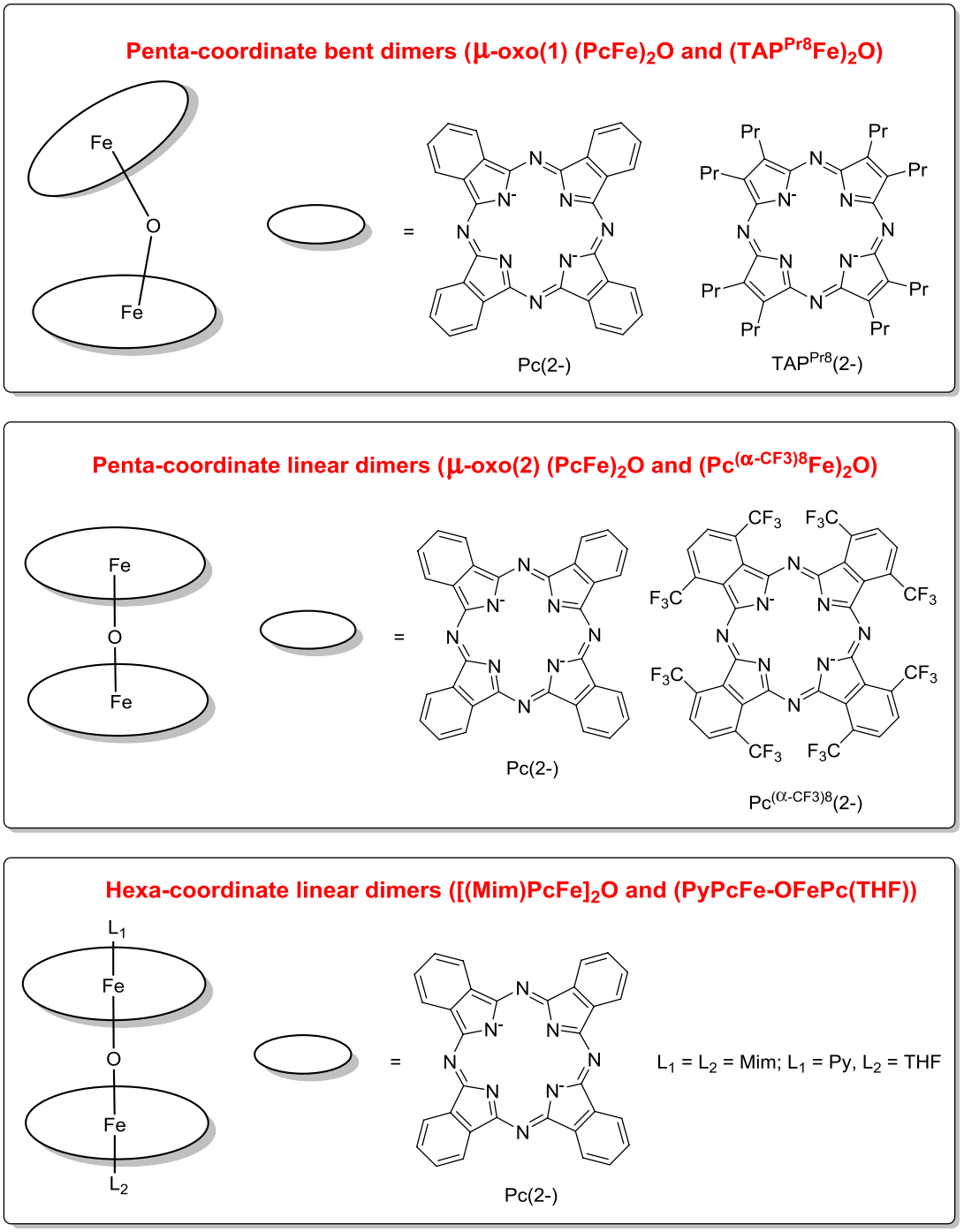

Fig. 1. Representative examples of crystallographically characterized (including this work) μ-oxo dimers of iron(III) phthalocyanines.

EXPERIMENTAL

X-ray crystallography

Single crystals of the μ-oxo(1) isomer of $(PcFe)_2O$ complex were accidentally obtained during the attempt to grow crystals of the $PcFe(NH_2NH\text{-}2Py)_2$ complex (where NH_2NH-2Py = 2-hydrazinopyridine) from DCM/hexanes solution. X-ray data were collected with a Mo micro source on a Bruker D8 Venture diffractometer at 100 K using an Oxford Cryostream low-temperature apparatus. Experimental data sets were reduced with Bruker SAINT. Absorption correction was done using SADABS [13]. The structure was solved using Superflip and refined using the SHELXTL program [14]. Disordered, partially occupied CH_2Cl_2 solvent observed in the pores of $(PcFe)_2O$ complex was eliminated with PLATON SQUEEZE [15] command. Complete structural data on the μ-oxo(1) isomer of $(PcFe)_2O$ complex can be accessed using CCDC reference number 2355475. They

are also available in the Supporting Information. In general, the small crystal size and its poor quality, does not allow us to reduce the R-factor below 10%.

DFT and TDDFT calculations

All calculations were run using Gaussian 16 [16]. BPW91 (pure GGA functional with 0% of Hartree-Fock exchange, [17]), TPSS (meta-GGA functional with 0% of Hartree-Fock exchange, [18]), TPSSh (hybrid functional with 10% of Hartree-Fock exchange, [18]), MPWLYP (hybrid functional with 5% of Hartree-Fock exchange, [19]), B3LYP (hybrid functional with 20% of Hartree-Fock exchange, [20]), and M05 (hybrid functional with 28% of Hartree-Fock exchange, [21]) exchange-correlation functionals were used in DFT calculations. Wachter's full-electron basis set [22] for iron and the 6-311G(d) basis set [23] for the other atoms were used for calculations. In all the DFT calculations stable=opt keyword was used to ensure the stability of the final wavefunction.

RESULTS AND DISCUSSION

Table 1 provides the information for the reported in the CCDC database μ-oxo dimers of iron(III) phthalocyanines. As it can be seen from Table 1, most of the reported systems have linear or nearly linear M-O-M geometries with the exceptions of reported here μ-oxo(1) dimer $(PcFe)_2O$ and $(TAP^{Pr8}Fe)_2O$ [24] complexes. As we have recently shown using Mössbauer spectroscopy and DFT calculations [12], the μ-oxo(1) isomer of $(PcFe)_2O$ complex is a more thermodynamically stable species in non-coordinating solvents, while the μ-oxo(2) isomer of $(PcFe)_2O$ complex can be stabilized and isolated in the solid state. Single crystals of μ-oxo(1) isomer of $(PcFe)_2O$ complex were obtained as one of the reaction products between PcFe(II) and 2-hydrazinopyridine, which is indicative of the oxidation of the PcFe(II) by the molecular oxygen during the catalytic cycle. The molecular structure of μ-oxo(1) isomer of $(PcFe)_2O$ complex is shown in Fig. 2.

It is commonly accepted that the degree of deviation of the transition-metal center from the N4 plane of porphyrin, phthalocyanine, or their analogs can be used to elucidate the spin state of such metal [28]. In the case of the μ-oxo(1) isomer of $(PcFe)_2O$ complex, the deviations from the N4 plane of the phthalocyanine ligand were calculated as 0.583 and 0.567 Å for Fe(1) and Fe(2) centers, respectively. These values are the largest for the phthalocyanine series and are indicative of the high-spin nature of the iron centers in this compound (Table 1). This observation agrees well with our recent DFT calculations on the same molecule according to which two iron(III) centers in the μ-oxo(1) isomer of $(PcFe)_2O$ complex are high-spin [12]. The closest analogs of μ-oxo(1) isomer of $(PcFe)_2O$ complex ($(TAP^{Pr8}Fe)_2O$ reported by Sorokin and co-authors [24] and perfluorinated $(Pc^{(\alpha\text{-}CF3)8}Fe)_2O$ reported by Gorun and co-authors [11]) have significantly smaller deviations of the iron centers from N4 plane (Table 1). The experimentally observed Fe-O-Fe angle in the μ-oxo(1) isomer of $(PcFe)_2O$ complex (152.44°) is also the smallest among known transition-metal phthalocyanine μ-oxo dimers with $(TAP^{Pr8}Fe)_2O$ complex having ~6° larger angle [24]. As we have demonstrated recently based on the DFT calculations, this might be reflective of the desire of two phthalocyanine ligands to maximize the π-π overlap between the individual π-systems, which would require a bent Fe-O-Fe structure [12]. The observed staggering angle between two phthalocyanine macrocycles (~24°) also supports this hypothesis. This angle is close to that reported for $(TAP^{Pr8}Fe)_2O$ system [24]. The competition between the steric strain caused by the bulky phthalocyanine ligands and the maximum overlap between π-clouds has already been discussed in detail [12]. On the other hand, bulky perfluorinated substituents in $(Pc^{(\alpha\text{-}CF3)8}Fe)_2O$ complex

Table 1. Summary of the crystal structures of penta- and hexa-coordinated μ-oxo iron(III) phthalocyanines.

Compound	CCDC	Fe-O, Å	Fe-N(av), Å[a]	Fe-O-Fe,°	Fe-N4, Å[b]	Staggered angle,°	Ref.
Penta-coordinated systems							
$(PcFe)_2O$ μ-oxo(1)	NA	1.79; 1.78	2.04; 2.04	152.4	0.58; 0.57	24.0	tw[c]
$(PcFe)_2O$ μ-oxo(1)	NA	1.79	2.07				[25][d]
$(PcFe)_2O$ μ-oxo(2)	NA	1.75	1.91	180	0.21		[10][e]
$(TAP^{Pr8}Fe)_2O$	TOSGAL	1.76; 1.75	1.94; 1.94	158.5	0.34; 0.37	24.2	[24]
$(Pc^{(\alpha\text{-}CF3)8}Fe)_2O$	DOTHUQ	1.76; 1.77	2.04; 2.04	178.4	0.2	31.5	[11]
Hexa-coordinated systems							
$[(Mim)PcFe]_2O$	KITPIM	1.75; 1.75	1.95; 1.95	175.1	0.02	42.5	[26]
(THF)PcFe-OFePc(Py)	KAVSAC	1.78(Py); 1.65(THF)	2.01; 2.01	178.8	0.04(Py); 0.33(THF)	38.6	[27]

[a]Average Fe-N bond distances for each iron center; [b]distance between the calculated N4 plane formed by the isoindole nitrogen atoms and iron(III) centers; [c]this work; [d]XANES/EXAFS analysis; [e]ADXD/EDXD analysis.

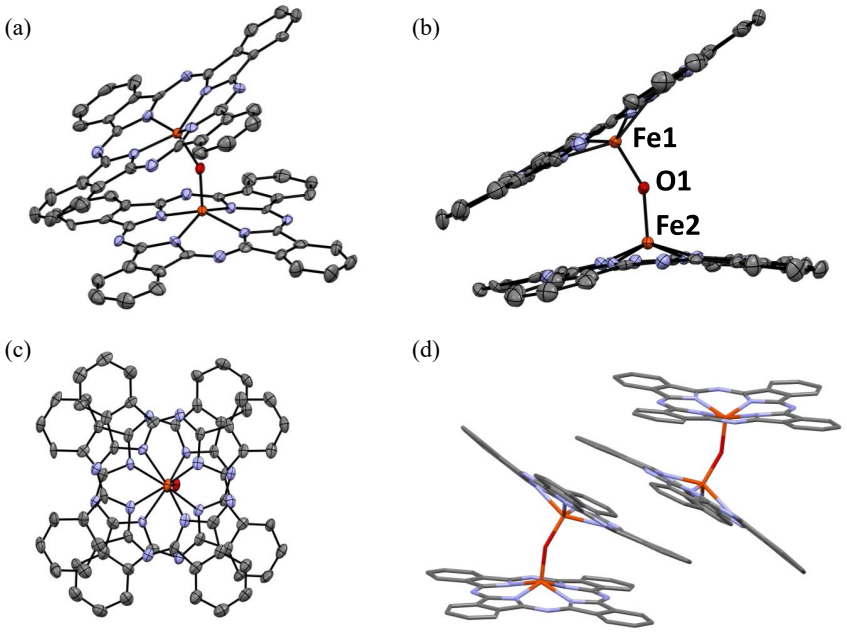

Fig. 2. X-ray crystal structure of μ-oxo(1) isomer of $(PcFe)_2O$ complex: (a) general view; (b) side-view; (c) top view; (d) unit cell packing. All figures have ellipsoids at 50% probability. In all cases, the hydrogen atoms are omitted for clarity.

[11] prevent bent structure formation and keep the Fe-O-Fe angle close to 180° (Table 1). Distortions caused by eight bulky CF_3 groups located at the α-positions of the phthalocyanine ligand increased the staggering angle to 31.5°. Interestingly, the staggering angle in the hexa-coordinated μ-oxo dimers are also larger (Table 1) [26, 27]. The bent structure of μ-oxo(1) isomer of $(PcFe)_2O$ complex also elongates Fe-O bond distances, which are the longest among currently known transition-metal μ-oxo dimers (Table 1). The average Fe-N bond distances in μ-oxo(1) isomer of $(PcFe)_2O$ complex are close to those observed in the perfluorinated $(Pc^{(\alpha\text{-}F3)8}Fe)_2O$ complex but a significantly longer compared to the other similar compounds in which iron centers are closer to N4 planes (Table 1). This is reflective of the larger deviation of the iron(III) centers from the N4 phthalocyanine plane. Both phthalocyanine ligands have bowl-shaped conformations with the center of the bowl pointing towards iron centers. The calculated depth of the bowl was defined as the interplanar distance between N4 planes and the planes formed by the furthest $Pc(C_\beta)$ atoms. The depths were found to be 0.609 and 0.276 Å for the first and the second phthalocyanine ligands, respectively.

As mentioned previously, all substituted μ-oxo(1) and μ-oxo(2) dimers are diamagnetic at room temperature [4, 12], while magnetism was studied for unsubstituted analogs [9]. Such diamagnetism required a strong antiferromagnetic coupling between two high-spin (confirmed by the X-ray crystallography discussed above) iron(III) centers. In the case, of unsubstituted μ-oxo(1) and μ-oxo(2) isomers, the experimentally determined antiferromagnetic coupling constants were reported as J = -120 and -195 cm^{-1}, respectively [29]. A significant bending of the Fe-O-Fe fragment in the μ-oxo(1) isomer of $(PcFe)_2O$ complex reduces the efficiency of the $Fe(d_{z2})$-$O(p_z)$-$Fe(d_{z2})$ magnetic superexchange pathway and increases the role of the out-of-plane $Fe(d_{yz},d_{xz})$-$O(p_z,p_y,p_x)$-$Fe(d_{yz},d_{xz})$ exchange pathways. In addition, as discussed previously in detail, d_{z2} and $d_{xz,yz}$ MOs can mix in the bent μ-oxo dimers, and thus all possible exchange pathways should be considered if one would like to estimate the overall magnitude of the antiferromagnetic coupling constant [30]. Although such a ligand-field-based process is very tedious, fortunately, modern DFT methods can directly handle such calculations [31]. Thus, we used the X-ray geometry of the μ-oxo(1) complex and several exchange-correlation functionals to estimate the magnitude of the antiferromagnetic coupling constant in this compound. First, in agreement with the previous calculations on the optimized geometries of μ-oxo(1) isomer of $(PcFe)_2O$ complex, our calculations using six different exchange-correlation functionals supported diamagnetic ground state (Table 2). The DFT-predicted low-spin to high-spin energy gap varies between ~32.5 and ~9.2 kcal/mol confirming the diamagnetic state of this dimer at room temperature.

We used Yamaguchi's formula [32] for the evaluation of coupling constant J in μ-oxo(1) isomer of $(PcFe)_2O$ complex as it covers both weak and strong coupling limit and was successfully applied in modeling of a large array of the dinuclear complexes using DFT methods: [33]

$$J = \frac{E_{HS} - E_{BS}}{\langle S^2 \rangle_{HS} - \langle S^2 \rangle_{BS}}$$

Table 2. Results of the Broken Symmetry (BS; antiferromagnetically couplet singlet states) versus High-Spin (HS; 11-et) DFT calculations using six different exchange-correlation functionals.

DFT method	ΔE (BS-HS), kcal/mol	J, cm^{-1}	Spin density (Fe1)	Spin density (Fe2)
BPW91/BS	32.5	-407	2.13	-2.12
BPW91/HS			4.05	4.03
TPSS/BS	29.6	-373	2.20	-2.19
TPSS/HS			4.07	4.06
MPWLYP/BS	15.3	-211	3.86	-3.84
MPWLYP/HS			4.04	4.03
TPSSh/BS	11.7	-162	4.02	-4.01
TPSSh/HS			4.16	4.15
B3LYP/BS	10.0	-138	4.06	-4.05
B3LYP/HS			4.16	4.15
M05/BS	9.2	-128	4.12	-4.11
M05/HS			4.21	4.20
Experiment		-120[29]		

Where E_{HS} and E_{BS} are DFT energies of the high-spin and broken-symmetry calculations and $\langle \hat{S}^2 \rangle$ values are the total spin angular momenta expectation values for Kohn-Sham determinants. The calculated values for the antiferromagnetic coupling constant decrease with the increase of the percentage of the Hartree-Fock exchange used in the exchange-correlation functional (Fig. 3). However, this change is not linear. One interesting observation from DFT calculations is that the DFT-predicted Mülliken spin densities using hybrid exchange-correlation functionals for the low-spin antiferromagnetically coupled states are close to four, which is expected for the high-spin iron(III) centers covalently bonded to the μ-oxo oxygen atom and extended π-system from the phthalocyanine ligand. This is also the case for all DFT calculations for the high-spin states (Table 2). However, in the broken-symmetry calculations of the diamagnetic state using pure exchange-correlation functionals, the Mülliken spin densities are close to two electrons, which puts spin states of iron(III) centers close to the intermediate spins (s = 3/2). This contradicts the X-ray-determined high-spin configuration of the iron(III) centers in μ-oxo(1) isomer of $(PcFe)_2O$ complex and thus, J-values obtained with the help of pure DFT exchange-correlation functionals cannot be trusted. In agreement with the previous DFT calculations [12], it seems that the B3LYP and M05 exchange-correlation functionals provide the closest agreement between theory and experiment. However, the experimentally determined J-values also should be treated with a grain of salt as unsubstituted μ-oxo(1) and μ-oxo(2) isomers of $(PcFe)_2O$ complex are very difficult to purify and they always have some amount of the paramagnetic monomeric impurities.

Another spectroscopic method that can clearly discriminate between the μ-oxo(1) and μ-oxo(2) isomers of the $(PcFe)_2O$ complex is Mössbauer spectroscopy. Indeed, although the isomer (IS) shifts for μ-oxo(1) and μ-oxo(2) isomers of $(PcFe)_2O$ complex are close to each other (ΔIS ~0.09–0.11 mm/s) [29], their quadrupole splittings (QS) are quite different (-0.44 mm/s for μ-oxo(1) and +1.38 for μ-oxo(2) isomers of $(Pc^{tBu4}Fe)_2O$ complex) [34]. Since the modern DFT methods can predict the Mössbauer quadrupole splittings with high accuracy [35], we tested these methods towards the prediction of the quadrupole splittings in μ-oxo(1) isomer of $(PcFe)_2O$ complex using the same six exchange-correlation functionals that we employed for the estimation of the antiferromagnetic coupling constants in this compound. The results of our calculations are listed in Table 3. Similar to the antiferromagnetic coupling constant calculation, all hybrid exchange-correlation functionals predict the correct sign and magnitude of the quadrupole splitting in the oxo(1) isomer of $(PcFe)_2O$ complex, while pure

Table 3. DFT-predicted Broken Symmetry (BS; antiferromagnetically couplet singlet states) quadrupole splitting in $(PcFe)_2O$ using six different exchange-correlation functionals.

DFT method	QS (Fe1), mm/s	QS (Fe2), mm/s	QS (average), mm/s
BPW91	+0.42	+0.43	+0.42
TPSS	+0.33	+0.34	+0.33
MPWLYP	-0.29	-0.36	-0.33
TPSSh	-0.30	-0.39	-0.35
B3LYP	-0.34	-0.44	-0.39
M05	-0.38	-0.48	-0.43
Experiment			-0.44[34]

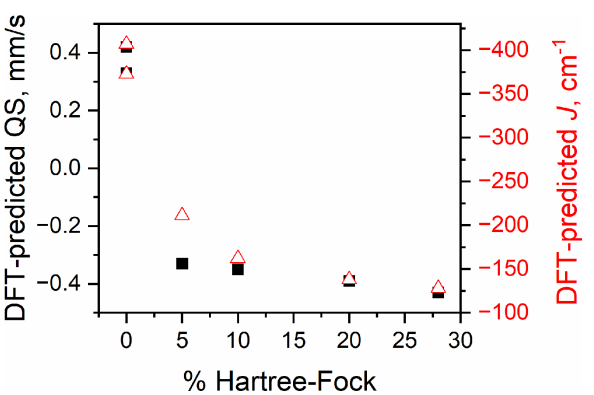

Fig. 3. DFT-predicted values for the antiferromagnetic coupling constants and quadrupole splittings in oxo(1) isomer of $(PcFe)_2O$ complex as a function of the Hartree-Fock exchange in the exchange-correlation functional.

DFT exchange-correlation functionals predict the incorrect sign of the quadrupole splitting. Interestingly, when overlayed with each other, the DFT graphs for the antiferromagnetic coupling constants and quadrupole splitting have very similar trends (Fig. 3) suggesting the importance of using the proper exchange-correlation functional with the correct amount of the Hartree-Fock exchange in the calculation of the spectroscopic properties of phthalocyanine dimers.

CONCLUSIONS

In this paper, we reported the structure of an illusive μ-oxo(1) isomer of the $(PcFe)_2O$ complex. The deviation of the two iron(III) centers from N4 planes formed by isoindole nitrogen atoms is indicative of their high-spin states. The Fe-O-Fe angle is the smallest known iron(III) phthalocyanine and tetraazaporphyrin μ-oxo dimers known so far. The DFT calculations on the μ-oxo(1) isomer of $(PcFe)_2O$ complex are indicative of the diamagnetic ground state. The antiferromagnetic coupling constant and Mössbauer quadrupole splitting in μ-oxo(1) isomer of $(PcFe)_2O$ complex are well reproduced by the hybrid exchange-correlation functionals. In contrast, the agreement between theory and DFT-predicted by the pure exchange-correlation functional values is rather poor.

Acknowledgments

Generous support from the NSF (CHE-2153081), Minnesota Supercomputing Institute, and the University of Tennessee to VN is greatly appreciated.

Supporting information

Crystallographic data have been deposited at the Cambridge Crystallographic Data Centre (CCDC) under the number CCDC-2355475. Copies can be obtained on request, free of charge, *via* https://www.ccdc.cam.ac.uk/structures/ or from the Cambridge Crystallographic Data Centre, 12 Union Road, Cambridge CB2 1EZ, UK (fax: +44 1223-336-033 or email: deposit@ccdc.cam.ac.uk)

REFERENCES

1. (a) Hanack M. in *Phthalocyanines: Properties and Applications*, Leznoff CC, Lever ABP. (Eds) VCH, New York, 1989; **2**: 43–96. (b) Taube R. *Pure Appl. Chem.* 1974; **38**: 427–438. (c) Ziegler CJ and Nemykin VN. *Dalton Trans.* 2023; **52**: 15647–15655. (d) Schrage BR, Zhou W, Harrison LA, Nevonen DE, Thompson JR, Prosser KE, Walsby CJ, Ziegler CJ, Leznoff DB and Nemykin VN. *Inorg. Chem.* 2022; **61**: 20177–20199. (e) Nevonen DE, Ferch LS, Schrage BR and Nemykin VN. *Inorg. Chem.* 2022; **61**: 8250–8266. (f) Nemykin VN, Nevonen DE, Osterloh WR, Ferch LS, Harrison LA, Marx BS and Kadish KM. *Inorg. Chem.* 2021; **60**: 16626–16644. (g) Nemykin VN, Kobayashi N, Chernii VY and Belsky VK. *Eur. J. Inorg. Chem.* 2001; **2001**: 733–743. DOI: 10.1002/1099-0682(200103)2001:3<733::AID-EJIC733>3.0.CO;2-2
2. (a) Canham GWR, Myers J and Lever ABP. *J. Chem. Soc. Chem. Commun.* 1973; 483–484. (b) Myers JF, Canham GWR and Lever ABP. *Inorg. Chem.* 1975; **14**: 461–468. (c) Schneider O and Hanack M. *Z. Naturforch.* 1984; **39b**: 265–267. (d) Hanack M, Hedtmann-Rein C, Datz A, Keppler U and Munz X. *Synthetic Metals* 1987; **19**: 787–792. (e) Silver J, Lukes P, Houlton A, Howe S, Hey P and Ahmet MT. *J. Mater. Chem.* 1992; **2**: 849–855. (f) Kalz W and Homborg H. *Z. Naturforch.* 1983; **38b**: 470–484. (g) Ough EA and Stillman MJ. *Inorg. Chem.* 1995; **34**: 4317–4325.
3. (a) Kennedy BJ, Murray KS, Zwack PR, Homborg H and Kalz W. *Inorg. Chem.* 1986; **25**: 2539–2545. (b) Ough EA. Ph.D. Thesis, University of Western Ontario, Canada, 1993, 232 pp. https://ir.lib.uwo.ca/cgi/viewcontent.cgi?article=3233&context=digitizedtheses. (c) Tiedemann MT and Stillman MJ. *J. Porphyrins Phthalocyanines* 2011; **15**: 1134–1149.
4. (a) Sievertsen S, Murray KS, Moubaraki B, Berry KJ, Korbatieh Y, Cashion JD, Brown LJ and Homborg H. *Z. Anorg. All. Chem.* 1994; **620**: 1203–1212. (b) Bakshi EN and Murray KS. Applied field Moessbauer spectra of low-spin mononuclear and binuclear iron(III)-phthalocyanines *Hyper. Inter.* 1988; **40**: 283–286. (c) Nemykin VN, Chernii VYa, Volkov SV, Bundina NI, Kaliya OL, Li VD and Lukyanets EA. *J. Porphyrins Phthalocyanines* 1999; **3**: 87–98. (d) Kennedy BJ, Murray KS, Zwack PR, Homborg H and Kalz W. *Inorg. Chem.* 1985; **24**: 3302–3305. (e) Frampton CS and Silver J. *Inorg. Chim. Acta* 1985; **96**: 187–191. (f) Ercolani C, Gardini M, Pennesi G and Rossi G. *J. Chem. Soc., Chem. Commun.* 1983; 549–550. (g) Dieing R, Schmid G, Witke E, Feucht C, Dressen M, Pohmer J and Hanack M. *Chem. Ber.* 1995; **128**: 589–598. (h) Ercolani C, Gardini M, Murray KS, Pennesi G, Rossi G and Zwack PR. *Inorg. Chem.* 1987; **26**: 3539–3543.
5. (a) Yamada Y, Miwa Y, Toyoda Y, Uno Y, Phung QM and Tanaka K. *Dalton Trans.* 2024; **53**: 6556–6567. (b) Yamada Y, Miwa Y, Toyoda Y, Phung QM, Oyama K and Tanaka K. *Catal. Sci. Technol.* 2023; **13**: 1725–1734. (c) Sorokin AB. *Adv. Inorg. Chem.* 2022; **79**: 23–63. (d) Afanasiev P and Sorokin AB. *Acc. Chem. Res.* 2016; **49**: 583–593. (e) Goedken VL and Ercolani C. *J. Chem. Soc., Chem. Commun.* 1984; 378–379. (f) Kennedy BJ, Murray KS, Homborg H and Kalz W. *Inorg. Chim. Acta* 1987; **134**: 19–21.

6. (a) Shimizu, T. Wakamatsu K, Yamada Y, Toyoda Y, Akine S, Yoza K and Yoshikawa H. *ACS Appl. Mater. Interfaces* 2021; **13**: 40612–40617. (b) Colomban C, Kudrik EV, Briois V, Shwarbrick JC, Sorokin AB and Afanasiev P. *Inorg. Chem.* 2014; **53**: 11517–11530. (c) Rossi G, Goedken VL and Ercolani C. *J. Chem. Soc., Chem. Commun.* 1988; 46–47. (d) Bakshi EN, Delfs CD, Murray KS, Peters B and Homborg H. *Inorg. Chem.* 1988; **27**: 4318–20. (e) Ercolani C, Gardini M, Goedken VL, Pennesi G, Rossi G, Russo U and Zanonato P. *Inorg. Chem.* 1989; **28**: 3097–3099. (f) Galich L, Kienast A, Hueckstaedt H and Homborg H. *Z. Anorg. Allg. Chemie* 1998; **624**: 1235–1242. (g) Zanotti G, Notarantonio S, Paoletti AM, Pennesi G and Rossi G. *J. Porphyrins Phthalocyanines* 2011; **15**: 748–755.
7. (a) Neu HM, Zhdankin VV and Nemykin VN. *Tetrahedron Lett.* 2010; **51** : 6545–6548. (b) Neu HM, Yusubov MS, Zhdankin VV and Nemykin VN. *Adv. Synth. Catal.* 2009; **351**: 3168–3174. (c) Geraskin IM, Luedtke MW, Neu HM, Nemykin VN and Zhdankin VV. *Tetrahedron Lett.* 2008; **49**: 7410–7412.
8. (a) Sorokin AB. *Chem. Rev.* 2013; **113**: 8152–8191. (b) Afanasiev P and Sorokin AB. *Acc. Chem. Res.* 2016; **49**: 583–593. (c) Sorokin AB, Kudrik EV, Bouchu D. *Chem. Commun.* 2008; 2562–2564.
9. (a) Ercolani C, Gardini M, Monacelli F, Pennesi G and Rossi G. *Inorg. Chem.* 1983; **22**: 2584–2589. (b) Ercolani C, Gardini M, Murray KS, Pennesi G and Rossi G. *Inorg. Chem.* 1986; **25**: 3972–3976.
10. Matassa R, Ballirano P, Donzello MP, Ercolani C, Sadun C and Caminiti R. *NANO* 2007; **2**: 121–128.
11. Gorun SM, Rathke JW and Chen MJ. *Dalton Trans.* 2009; 1095–1097.
12. Nemykin VN, Schrage BR, Nevonen DE, Harrison LA, Newman KME, Paidi VK and van Lierop J. *Inorg. Chem.* 2023; **62**: 10203–10220.
13. Palatinus L and Chapuis G. *J. Appl. Cryst.* 2007; **40**: 786–790.
14. Sheldrick GM. *Acta Cryst.* 2008; **A64**: 112–122.
15. Spek AL. 2005 A Multipurpose Crystallographic Tool. Utrecht University. Utrecht. The Netherlands.
16. *Gaussian 16, Revision B.01*, Frisch MJ, Trucks GW, Schlegel HB, Scuseria GE, Robb MA, Cheeseman JR, Scalmani G, Barone V, Petersson GA, Nakatsuji H, Li X, Caricato M, Marenich AV, Bloino J, Janesko BG, Gomperts R, Mennucci B, Hratchian HP, Ortiz JV, Izmaylov AF, Sonnenberg JL, Williams-Young D, Ding F, Lipparini F, Egidi F, Goings J, Peng B, Petrone A, Henderson T, Ranasinghe D, Zakrzewski VG, Gao J, Rega N, Zheng G, Liang W, Hada M, Ehara M, Toyota K, Fukuda R, Hasegawa J, Ishida M, Nakajima T, Honda Y, Kitao O, Nakai H, Vreven T, Throssell K, Montgomery JA Jr, Peralta JE, Ogliaro F, Bearpark MJ, Heyd JJ, Brothers EN, Kudin KN, Staroverov VN, Keith TA, Kobayashi R, Normand J, Raghavachari K, Rendell AP, Burant JC, Iyengar SS, Tomasi J, Cossi M, Millam JM, Klene M, Adamo C, Cammi R, Ochterski JW, Martin RL, Morokuma K, Farkas O, Foresman JB and Fox DJ. *Gaussian, Inc.*, Wallingford CT, 2016.
17. (a) Becke AD. *Phys. Rev. A*. 1988; **38**: 3098–3100. (b) Perdew JP. *Phys. Rev. B*. 1986; **33**: 8822–8824.
18. (a) Staroverov VN, Scuseria GN, Tao J and Perdew JP. *J. Chem. Phys.* 2003; **119**: 12129–12137. (b) Tao JM, Perdew JP, Staroverov VN, Scuseria GE. *Phys. Rev. Lett.* 2003; **91**: 146401.
19. Schultz NE, Zhao Y and Truhlar DG. *J. Phys. Chem. A* 2005; **109**: 11127–11143.
20. (a) Becke AD. *J. Chem. Phys.* 1997; **107**: 8554–8560. (b) Becke AD. *J. Chem. Phys.* 1993; **98**: 5648–5652.
21. Zhao Y and Truhlar DG. *Theor. Chem. Acc.* 2008; **120**: 215–241.
22. Wachters AJH. *J. Chem. Phys.* 1970; **52**: 1033–1036.
23. McLean AD and Chandler GS. *J. Chem. Phys.* 1980; **72**: 5639–5648.
24. Colomban C, Kudrik EV, Tyurin DV, Albrieux F, Nefedov SE, Afanasiev P and Sorokin AB. *Dalton Trans.* 2015; **44**: 2240–2251.
25. Choi HJ, Kwag G and Kim S. *J. Electroanalytical Chem.* 2001; **508**: 105–114.
26. Ercolani C, Monacelli F, Dzugan S, Goedken VL, Pennesi G and Rossi G. *J. Chem. Soc. Dalton Trans.* 1991; 1309–1315.
27. Lin M-J, Wang J-D, Chen N-S and Huang J-L. *Inorg. Chem. Commun.* 2005; **8**: 900–902.
28. (a) Zhou Z, Shen M, Cao C, Liu Q and Yan Z. *Chem. Eur. J.* 2012; **18**: 7675–7679. (b) Rydberg P and Olsen L. *J. Phys. Chem. A* 2009; **113**: 11949–11953. (c) Ohgo Y, Saitoh T and Nakamura M. *Acta Crystallog., Section C* 2001; **C57**: 233–234. (d) Tang SC, Koch S, Papaefthymiou GC, Foner S, Frankel RB, Ibers JA and Holm RH. *J. Am. Chem. Soc.* 1976; **98**: 2414–2434. (e) Ercolani C and Floris B. in: *Phthalocyanines: Properties and Applications* Leznoff CC, Lever ABP (Eds), VCH 1996; **4**: 405–425.
29. Ercolani C and Floris B. in: *Phthalocyanines: Properties and Applications* Leznoff CC, Lever ABP (Eds), VCH 1993; **2**: 3–41.
30. Brown CA, Remar GJ, Musselman RL and Solomon EI. *Inorg. Chem.* 1995; **34**: 688–717.
31. (a) Costa IFM, Franco CHJ, Nesterov DS, Andre V, Pereira LCJ and Kirillov AM. *J. Phys. Chem. C* 2024; **128**: 6053–6064. (b) Benediktsson B and Bjornsson R. *J. Chem. Theory Comput.* 2022; **18**: 1437–1457. (c) Vassilyeva OYu, Buvaylo EA, Kokozay VN, Skelton BW, Sobolev AN, Bienko A and Ozarowski A. *Dalton Trans.* 2021; **50**: 2841–2853.

(d) Premuzic D, Holynska M, Ozarowski A, Pietzonka C, Roseborough A and Stoian SA. *Inorg. Chem.* 2020; **59**: 10768–10784.
32. Yamanaka S, Kawakami T, Nagao H and Yamaguchi K. *Chem. Phys. Lett.* 1994; **231**: 25–33.
33. Pantazis DA, Krewald V, Orio M and Neese F. *Dalton Trans.* 2010; **39**: 4959–4967.
34. Ravikanth R, Achim C, Tyhonas JS, Münck E and Lindsey JS. *J. Porphyrins Phthalocyanines* 1997; **1**: 385–394.
35. (a) Nemykin VN, Nevonen DE, Ferch LS, Shepit M, Herbert DE and van Lierop J. *Inorg. Chem.* 2021; **60**: 3690–3706. (b) Nemykin VN and Hadt RG. *Inorg. Chem.* 2006; **45**: 8297–8307. (c) Zhang Y, Mao J, Godbout N and Oldfield E. *J. Am. Chem. Soc.* 2002; **124**: 13921–13930. (d) Han W-G, Liu T, Lovell T and Noodleman L. *J. Comput. Chem.* 2006; **27**: 1292–1306. (e) Roemelt M, Ye S and Neese F. *Inorg. Chem.* 2009; **48**: 784–785. (f) Papai M and Vanko G. *J. Chem. Theory Comput.* 2013; **9**: 5004–5020.